Applied Energy 221 (2018) 464–476

Contents lists available at ScienceDirect

Applied Energy

journal homepage: www.elsevier.com/locate/apenergy

Mathematical modelling of operation modes and performance evaluation of an innovative small-scale concentrated solar organic Rankine cycle plant

Luca Cioccolanti[a,*], Roberto Tascioni[a], Alessia Arteconi[a]

[a] Università Telematica e-Campus, Via Isimbardi 10, 22060 Novedrate, CO, Italy

HIGHLIGHTS

- An innovative small scale concentrated solar ORC has been modelled using TRNSYS.
- The performance of the system have been evaluated under a given control strategy.
- Different operating modes of the systems are analysed during one year period;
- At high DNI the plant is able to achieve performance close to the design ones.
- The simulation analysis provides insights for the subsequent testing of the real plant.

ARTICLE INFO

Keywords:
Simulation analysis
Renewable energy
Micro combined heat and power plant
Concentrated solar power
ORC system
Residential applications

ABSTRACT

In this paper an innovative small-scale concentrated solar 2 kWe organic Rankine cycle plant coupled with a phase change material storage tank equipped with reversible heat pipes is investigated using a simulation analysis. The plant, intended for residential applications, is going to be built and tested under the European funded H2020 Innova MicroSolar project executed by the consortium of several Universities and industrial organizations, led by Northumbria University. The authors of this work used the design of the integrated system, developed by the consortium, to preliminary estimate the overall performance of the system in order to provide useful information for its forthcoming real operation. In particular, according to the varying ambient conditions, the influence of different operation modes of the prototype plant are evaluated. The dynamic simulation analysis has shown an interesting performance of the system in terms of annual operating hours, power production and conversion efficiencies. More precisely, the organic Rankine cycle unit is able to operate for more than 3100 h/year, achieving the design performance when solar power is sufficiently high, producing about 5100 kWh_e/year. For the considered operating set-point temperatures of the thermal energy storage, the plant is able to reach high conversion efficiency also when the organic Rankine cycle unit is supplied by discharging the energy stored in the storage tank, for about 800 h/year. Hence, the work has provided some useful insights into the best working conditions of such micro combined heat and power system to be integrated in residential buildings. Moreover, the analysis could serve as a general guide for the design and optimization of the mutual interactions of the different subsystems in small-scale concentrated solar organic Rankine cycle plants.

1. Introduction

In order to achieve the ambitious and challenging climate goals set by the Paris Agreement [1] that entered into force on October 2016, breakthrough energy technologies and innovation are recognized of paramount importance. Irrespective of any tangible climate change mitigation agreement, renewable sources have a key role in reducing greenhouse gas emissions, thus contributing to a sustainable development [2]. In 2015 renewable power generation increased by about 5% and it accounted for around 23% of the overall electricity generation worldwide [3]. Energy from the sun is by far the major source of renewable energy and about $1 \cdot 10^5$ TW reaches the surface of the earth. Therefore, solar energy is available in many regions and represents the most promising and clean energy for future power generation [4]. In particular, Concentrated Solar Power (CSP) technologies are foreseen as a valuable alternative to substitute thermal and electric power generation from fossil fuel. These technologies are able to concentrate sunlight from a large area onto a smaller one by means of optical devices like lenses or mirrors. The concentrated light is then collected using a solar receiver and converted into electric or thermal power

* Corresponding author.
E-mail addresses: luca.cioccolanti@uniecampus.it (L. Cioccolanti), roberto.tascioni@uniecampus.it (R. Tascioni), alessia.arteconi@uniecampus.it (A. Arteconi).

https://doi.org/10.1016/j.apenergy.2018.03.189
Received 31 December 2017; Received in revised form 30 March 2018; Accepted 31 March 2018

Nomenclature

A	area of the primary collectors [m^2]
c_1	first order heat losses coefficient [kW/m C]
c_4	fourth order heat losses coefficient [kW/m C^4]
CAPEX	capital expenditure [€]
CPC	Compound Parabolic Collector
CHP	Combined Heat and Power
CSP	Concentrated Solar Power
DNI	Direct Normal Irradiation [kW/m^2]
dr	discount rate [%]
IAM	Incident Angle Modifier
h_{ORC}	operating hours of the ORC unit [h]
L_{abs}	length of the absorber tubes [m]
LCOE	Levelized Cost of Electricity [€/kWh_e]
LFR	Linear Fresnel Reflector
OM	Operation Mode
ORC	Organic Rankine Cycle
Eff_{LFR}	overall conversion efficiency of the LFR solar field [%]
Eff_{TES}	efficiency of TES [%]
$Eff_{ORC,el}$	electric efficiency of the ORC unit [%]
$Eff_{ORC,th}$	thermal efficiency of the ORC unit [%]
$Eff_{ORC,tot}$	overall efficiency of the ORC unit [%]
Eff_{TOT}	total conversion efficiency of the plant [%]
E_{gen}	electric energy generated [kWh_e]
ir	inflation rate [%]
$\dot{m}_c$	mass flow rate of the cooling water [kg/s]
$\dot{m}_f$	mass flow rate of the organic fluid [kg/s]
OPEX	operating expenditure [€]
PCM	Phase Change Material
$P_{LFR,in}$	inlet power to the LFR [kW]
$P_{LFR,out}$	outlet thermal power from the LFR [kW_t]
$P_{LFR,peak}$	peak outlet thermal power from the solar field [kW_t]
$P_{TES,in}$	inlet thermal power to the TES [kW_t]
$P_{ORC,in}$	inlet thermal power to the ORC [kW_t]
$P_{ORC,in,n}$	nominal inlet thermal power to the ORC [kW_t]
$P_{ORC,out}$	outlet thermal power from the ORC [kW_t]
$P_{ORC,el}$	electric power produced by the ORC [kW_e]
PV	Photovoltaic
PTC	Parabolic Trough Collectors
Q_{loss}	heat losses at the receiver [kW_t]
Q_{PCM}	heat exchanged by the PCM [kW_t]
SM	Solar Multiple
TES	Thermal Energy Storage
T_{abs}	average temperature of the absorber tube [°C]
$T_{LFR,out}$	outlet temperature of the diathermic oil from the LFR solar field [°C]
T_{oil}	temperature of the diathermic oil [°C]
$T_{ORC,in}$	inlet temperature of the diathermic oil to the ORC [°C]
$T_{ORC,off}$	lower bound temperature set-point of the TES [°C]
$T_{ORC,on}$	upper bound temperature set-point of the TES [°C]
$T_{TES,av}$	average temperature of the TES [°C]
$T_{TES,max}$	maximum temperature of the TES [°C]
T_{in}	inlet temperature of the cooling water at the condenser [°C]
T_{out}	outlet temperature of the cooling water at the condenser [°C]
Δh_e	actual specific enthalpy difference across the expander [kJ/(kg K)]
Δh_p	actual specific enthalpy difference across the pump [kJ/(kg K)]
ΔT_{PCM}	temperature difference between the PCM and the heat transfer medium [°C]
$\Delta t_{int\text{-}timestep}$	time interval of the internal time step [s]

Greek symbols

α	solar elevation angle
ε	emittance coefficient
η_{el}	electric efficiency
η_m	mechanical efficiency
η_{opt}	optical efficiency
$\eta_{opt,max}$	maximum optical efficiency
η_{rec}	efficiency receiver factor
σ	solar azimuthal angle
θ	solar incident angle

depending on the temperature level and the plant scale. Among the different CSP technologies, Linear Fresnel Reflectors (LFRs) proved to be a very promising solution as solar concentrator for medium and high temperature thermal applications thanks to their potential to overcome techno-economic constraints associated with conventional reflector based CSP [5]. Compared to Parabolic Trough Collectors (PTC) indeed LFRs show a great potential for cost reduction, thanks to a lighter structure and a fixed receiver, which can be designed for optimum integrated thermal performance [6]. At present, for an installed power lower than few hundreds of kW, the specific cost of a LFR solar field is about 200 €/m^2 of collector area [7], but it can be reduced up to 150 €/m^2 in case of system improvements and large scale production [8]. Although the benefits of their usage in building-façade for power generation have been proven [9], their adoption in buildings has been limited so far. In fact, at residential level evacuated tubes are preferred, because of their ease of installation and absence of tracking mechanisms. However, the use of medium and high temperature solar technologies in buildings can be economical and feasible if the systems are designed reasonably [10], because of the high potential of cogeneration at residential scale [9] where both thermal and electric energy are requested. To efficiently convert solar energy into generated power, Organic Rankine Cycle (ORC) systems are considered as one of the most common and competitive technologies [11]. An Organic Rankine Cycle plant works similarly to a Rankine steam power plant, but it makes use of organic working fluids which are able to condense and evaporate at acceptable temperatures [12]. On large scale, several manufacturing companies for ORC exist and their products are already into the market [13]. However, different factors are boosting the interest for small ORC units, such as the need of power in developing countries, the request of polygeneration systems for grid connected applications in developed countries as well as the deregulation and privatization of the electric generation sector worldwide [12]. There are still several challenges for the exploitation of low grade thermal energy resources by means of ORC systems [14], therefore, also academic research is paying a lot of attention on them. For example, Bouvier et al. [15] experimentally investigated the performance of a micro Combined Heat and Power (CHP) system composed of a solar PTC coupled to a steam Rankine cycle expander for direct steam generation. Although low output electric power and solar-to-electricity efficiency are achieved, the analysis showed the feasibility of adopting such a system for hot water or heating production into a building. Taccani et al. [16] tested a small-scale micro solar CHP (< 10 kWe) powered by parabolic trough solar collectors with a collector surface area of 100 m^2. They indicated that the system can achieve 8% as gross electricity efficiency. Instead, Xu et al. [17] evaluated the performance of a LFR-ORC system through a theoretical and simulation study. Results showed that the supercritical ORC system is better than the subcritical one independently from the considered working fluid. Antonelli et al. [18] carried out a dynamic modelling of a low concentration solar plant consisting of static compound parabolic collectors coupled with an ORC unit in AMEsim. The

authors found that the use of a volumetric expansion device with variable rotational speed allows operation without need of any storage system. However, in order to increase the annual energy production of a small-scale solar ORC, a Thermal Energy Storage (TES) tank is usually employed. TES plays a key role to ensure the normal operation of such systems by reducing the effect of the variable solar radiation as addressed by several studies. Freeman et al. [19], for example, stated that a thermal energy storage is a key feature for their domestic solar-ORC combined heat and power system for year-round operation in the UK, in order to buffer the intermittent input of solar thermal energy to the system. Li et al. [20] analysed the dynamic performance of a solar ORC with TES, finding that a proper TES capacity, which allows to suppress the dynamic impact of solar fluctuations and avoid resonance phenomena in the plant, exists. Even He et al. [21] developed a transient simulation model of a PTC solar field coupled with a single tank TES and an electricity conversion system based on ORC focusing on the effects of several key parameters. In particular, the influence of the volume of the TES on the performance of the system has been considered and its optimal volume with seasonality assessed. Freeman et al. [22] compared sensible and latent TES for a domestic-scale solar combined heat and power system. They found that a 20% higher total daily electric output per unit storage volume can be achieved with a Phase Change Material (PCM) storage compared to a water energy storage. Moreover, the isothermal operation of the PCMs during phase change allows for higher energy conversion efficiencies. Manfrida et al. [23], instead, developed a mathematical model of a TES containing PCM and evaluated its application in a solar power ORC over one week period. In particular, results showed that the proposed plant is able to generate power for almost 80% of the simulated period with a weekly average overall solar-to-electricity efficiency of 3.9%. At the same time, the analysis revealed that appropriate control logics are required to improve the performance of the system over a more extended period. An adequate modelling of the different subsystems and the optimal design of the operational strategies of such systems are indeed of paramount importance to achieve higher conversion efficiency and annual performance. For example, in waste heat recovery ORC cycle, second law efficiency can be improved by about 10% by implementing a proper control strategy which takes into account the heat source variability [24]. In particular, Hernandez et al. [25] designed and experimentally validated an adaptive model predictive control law to optimally recover waste heat with a ORC unit. The analysis proved that the proposed control outperforms the gain-scheduled PID strategy and allows regulating accurately the superheating at the evaporator outlet. When a TES unit is also included in the plant, optimal design of subsystems and their interactions are fundamental. Petrollese and Cocco [7] evaluated the optimal design parameters of a hybrid LFR coupled with a TES system, an ORC plant and a PV array to follow a constant output power level for different daily time periods. Patil et al. [26], instead, carried out a techno-economic comparison of the performance of a small scale concentrated solar ORC with the performance of a photovoltaic (PV) plant, taking into account their coupling with energy storage systems. In particular, the analysis showed that both systems achieve the minimum levelized cost of electricity (LCOE) when no storage is included and the solar ORC with storage is more competitive than PV when reliability of power supply is the most important factor to guarantee. Barbieri et al. [27] analysed the feasibility of micro-CHP systems to meet the household energy demands of single family users, while Bianchi et al. [28] evaluated the profitability of different micro-CHP systems consisting of prime mover, auxiliary boiler, TES and electric energy storage system for residential applications. The optimum number of electric energy storage modules, their specific costs and the maximum number of shut down for each prime mover technology (including micro ORC) have been evaluated according to the Italian scenario. Calise et al. [29] investigated the energy and economic performance of a 6kWe ORC unit coupled with 73.5 m^2 of innovative flat-plate evacuated solar collectors in different climatic conditions. They showed that while the efficiency of the ORC does not vary significantly during the year, the efficiency of solar collectors is high in summer, but very low in winter. The economic feasibility of such a system is possible in presence of feed-in tariff incentive schemes.

Given the interest towards solar heat and power systems and their potential to be used also at small-scale, as shown by the above literature review, in this paper a micro solar ORC plant for residential applications is considered. Purpose of the work is to analyse an innovative integration of the best available technologies, in order to highlight its positive and negative aspects and to provide indications to overcome the barriers for the uptake of such systems. With more detail, a small-scale 2kWe Organic Rankine Cycle system coupled with a concentrated solar LFR plant and a PCM thermal storage system equipped with reversible heat pipes is considered. The conceptual idea of the plant has been first proposed by researchers at Northumbria University and a prototype plant has been designed and will be tested by the whole consortium under the Innova MicroSolar EU project [30], led by Northumbria University. To the best of the authors' knowledge, at such small scale a detailed analysis for a similar configuration has not been already investigated in literature. Apart from the system configuration, the main novelty of the present work lies in the evaluation of the performance of the prototype plant under a given control strategy, conceived to improve the exploitation of the available solar energy for the main purpose of electricity production. Different operating modes of the systems indeed are analysed during one year period by means of a simulation model representing the prototype plant.

Therefore, the paper is organized as follows: after the Introduction, Section 2 describes the general features of the prototype plant; Section 3 reports a description of the simulation model developed while Section 4 presents and discusses the main results of the work. Finally, Section 5 reports the conclusions.

2. Plant description

The system under analysis is an innovative micro-Combined Heat and Power (m-CHP) plant, which is being developed by the consortium of several Universities and industrial organizations, led by Northumbria University, with the funding from EU under the Innova MicroSolar Project [30], which involves 3 universities, 5 small and medium enterprises and 1 corporation. As first proposed by Northumbria University and then developed by the partners of the project, the plant consist of: (i) a concentrated LFR solar field producing heat at temperatures in the range 250–280 °C; (ii) a 2 kWe/18 kWt Organic Rankine Cycle plant; (iii) an advanced PCM thermal storage tank equipped with reversible heat pipes and (iv) a domestic boiler for hot water and space heating for application in households and small business residential buildings. Purpose of this EU funded project is to develop an innovative high performance and cost effective solar heat and power system with the final aim of encouraging the uptake of renewable heat technologies. Thus the technologies involved have been chosen in order to fulfill such target and obtain a good trade-off between performance and costs.

More precisely, the solar field is made up of 2 adjacent LFR modules. LFR technology is particularly suitable as solar collector at small-scale, because it allows to build modular systems, more flexible and less cumbersome than other collectors (e.g. PTC), thus LFR modules can be adapted to different geometries, as requested in residential applications, with a good compromise between costs and accuracy. The LFR collector has a total length of about 20 m, a ground area of around 240 m^2 and a net mirror surface area of about 146 m^2. The receiver, placed at about 3.5 m from the ground, consists of evacuated tube collectors with a thermal conversion efficiency of nearly 90% and a maximum operating temperature of 400 °C. A Concentrated Parabolic Compound (CPC) secondary receiver redirects towards the receiver a small portion of the beams that otherwise would not hit the receiver tubes. The peak thermal power of the solar field is about 80 kW at

nominal operating conditions (DNI equal to 900 W/m^2) as designed by the manufacturing company [8]. The Solar Multiple (SM) of the plant, defined as in Eq. (1):

$$SM = P_{LFR,peak}/P_{ORC,in,n} \quad (1)$$

where $P_{LFR,peak}$ is the peak output thermal power from the solar field and $P_{ORC,in,n}$ the nominal input power of the ORC unit, is equal to 3.63.

The ORC unit developed and manufactured by ENOGIA [31] operates accordingly to a regenerative cycle using NOVEC 649 as working fluid. The fluid is a nonflammable, non-toxic segregated hydrofluoroether combining excellent thermal stability and outstanding environmental properties [32]. The fluid exits the evaporator with a superheating of 5 °C to prevent any liquid at the expander inlet and expands in an axial turbine to theoretically achieve a gross electric power production and conversion efficiency of the plant equal to 2.38 kWe and 10.8% respectively. Then, the organic working fluid passes through the regenerator and the condenser where its subcooling, necessary to guarantee only liquid at the pump inlet, is limited to 1 °C. Finally, a pump increases the fluid pressure up to 18 bar maximum. Depending on the ambient conditions, the working fluid is heated up in the evaporator using directly the energy collected by the LFR solar field or the thermal energy stored by the storage tank.

The considered energy storage system (with PCM and heat pipes) allows to achieve a high specific heat accumulation capacity and a reduced charging/discharging time. The PCM storage tank, designed by Northumbria University [33] and Aavid Thermacore [34], is made of nitrate solar salt kNO_3(40 wt%)/$NaNO_3$(60 wt%), which has a high heat of fusion but a low thermal conductivity. About 3.8 tons of this material in a 1.93 m^3 tank is needed to store about 100 kWh of latent thermal energy from the solar field in order to guarantee 4 h of ORC unit operation during night time with a nominal input power of 25 kW. Reversible heat pipes, developed by Aavid Thermacore [34], are able to transfer heat both from the solar field to the storage tank and from the latter to the ORC unit depending on the operating conditions (charging or discharging). These pipes, charged with a sufficient amount of demineralized water to carry the required power, are able to withstand a maximum pressure of 100 bar. They are located to ensure that all the PCM volume is heated and cooled equally without hot or cold spots that would sensibly reduce the heat transfer performance. The central control system for the plant is developed by S.TRA.TE.G.I.E. srl [35].

3. Model description

The dynamic simulation model of the prototype plant presented above has been developed by the authors in TRNSYS [36], which allows to predict the dynamic performance of complex energy systems. In particular, the following main components have been considered: (i) a LFR solar field; (ii) a micro ORC plant; (iii) a PCM thermal energy storage tank equipped with reversible heat pipes; (iv) pipes connecting the main components. In this representation the plant is operated to produce electricity at its maximum and the thermal load is considered as a by-product which can be entirely collected and used by final users. Therefore a detailed heating demand has not been assumed and the domestic hot water boilers have not been included in the model at this stage. Fig. 1 reports a scheme of the system under consideration.

Despite TRNSYS library has a wide range of types for the simulation of many components, specific subroutines for the LFR solar field, the ORC unit and the PCM storage tank equipped with heat pipes have been developed by the authors in Matlab [37] and then coupled with the simulation environment in TRNSYS [36]. In this way, the peculiar characteristics of each subsystem is represented into the model.

3.1. LFR solar field model

The solar field has been modelled as operating under quasi-steady state conditions. The most important aspect to predict the performance of a LFR solar collector is its optical efficiency, which depends on several parameters. The geometry of the collectors, the material of the reflecting and absorbing surfaces as well as the sun shape, which varies with time and location, are the main factors. The solar incident angle (θ) is expressed in terms of the solar elevation angle (α) and the azimuthal angle (σ). The former is the angle between the horizontal plane and the sun direction, while the latter is the angle measured from the azimuth reference direction (y-axis) to the perpendicular projection of the sun direction on the reference plane. Fig. 2 shows the position of the sun with respect to the solar elevation and azimuthal angles.

A ray tracking mechanism allows focusing the solar rays on the receiver surface according to the position of the sun. In order to increase the flux hitting the receiver and the related concentration ratio, secondary reflectors are used to reflect the rays from the primary collectors onto the surface of the absorber. However, both cosine losses and shading and blocking effects contribute to limit the optical

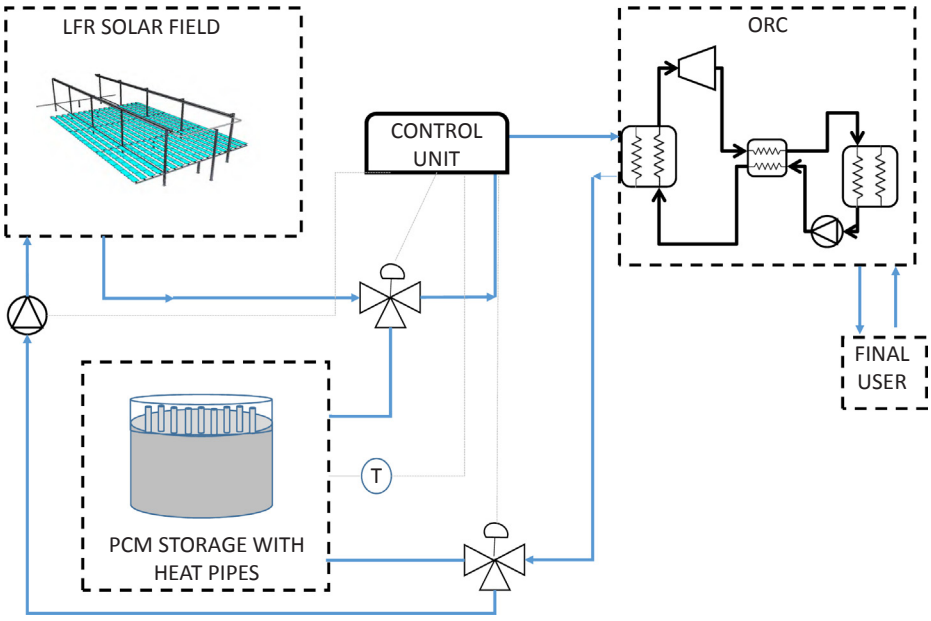

Fig. 1. Schematic of the integrated system under analysis.

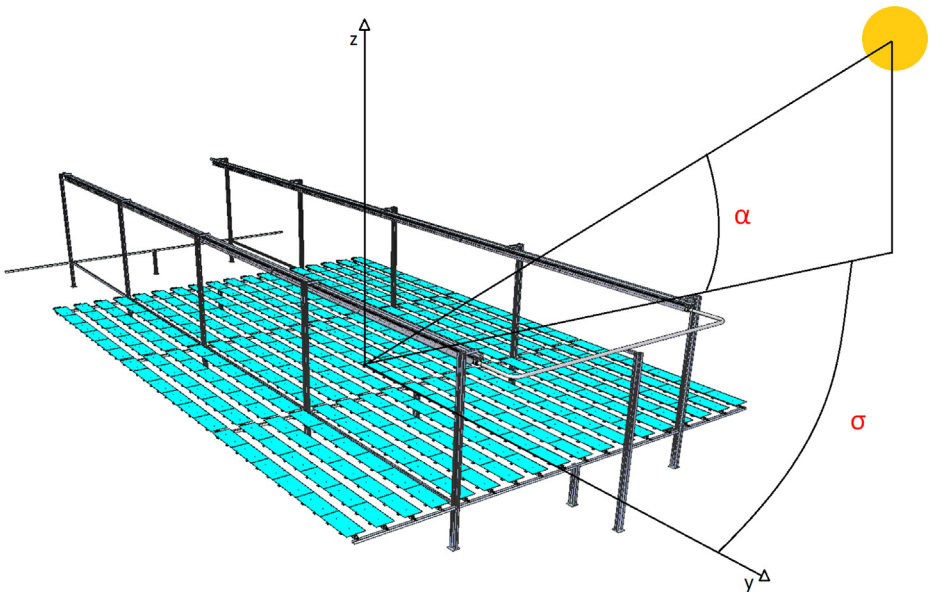

Fig. 2. Relative position of the sun and the collector.

efficiency of the LFR. In order to take into account the influence of the incident angle on the optical performance of the system, the maximum optical efficiency, which is achieved when the incident angle is zero, is multiplied by the Incident Angle Modifier (IAM) as reported in Eq. (2):

$$\eta_{opt} = \eta_{opt,max}(\theta = 0)\cdot IAM(\alpha,\sigma) \quad (2)$$

where the IAM values of the collector under analysis have been provided by the manufacturing company ELIANTO [8] at different solar elevation and azimuthal angles.

In turn, the collected thermal energy depends also on the heat losses at the receiver which are independent from the collector. For vacuum receivers operating in the temperature range 100–600 °C the heat losses can be evaluated as in Eq. (3) [38]:

$$Q_{loss} = (c_1\cdot T_{abs} + c_4\cdot T^4)\cdot L_{abs} \quad (3)$$

where L_{abs} is the length of the absorber tubes, T_{abs} the average temperature of the absorber, while the coefficients c_1 and c_4 depend on the aperture width of the absorber and the DNI. Considering the contribution of the cosine effect while neglecting the thermal capacity of the collectors, the collected thermal energy is evaluated as in Eq. (4):

$$P_{LFR,out} = A\cdot DNI\cdot\cos(\theta)\cdot\eta_{opt}\cdot\eta_{rec} - Q_{loss} \quad (4)$$

where A is the area of the primary collectors, cos(θ) the cosine of the solar incident angle and η_{rec} the receiver efficiency. Paratherm NF oil is used as heat transfer fluid to deliver heat to the rest of the plant. The oil flow rate is adjusted in order to keep the oil temperature at 210 °C when the solar field supplies the ORC, in order to maintain a good electric conversion efficiency (see Section 3.2, Fig. 3), or at 10 °C more than the average TES temperature when the solar field supplies the storage (see Section 3.5).

3.2. ORC model

Depending on the ambient conditions, the ORC receives the input thermal power by the LFR solar field, by the TES or by a combination of both (see Section 3.5). In this work, the ORC has been modelled considering steady state conditions. The following assumptions, based on the design specifications, have been made: the temperature difference between the inlet oil from the plant (LFR and or TES) and the organic fluid evaporating temperature is constant and equal to 34 °C if the cycle is subcritical (i.e. the resulting evaporating temperature remains below the organic fluid critical temperature, otherwise the evaporating temperature is set 5 °C lower than the critical temperature). At the evaporator outlet a minimum superheating of 5 °C is considered while at the condenser outlet the working fluid is at saturated conditions (no subcooling). Pressure drops in the components have been neglected.

The pump and turbine isentropic efficiencies vary with operating conditions according to the data provided by the manufacturer, ENOGIA [31], while the generator electric efficiency has been assumed equal to 0.9 and the mechanical efficiency to 0.95. The overall heat transfer efficiency of the heat exchangers has been assumed constant, given by the manufacturer design data. In particular, the evaporator has been modelled according to the ε-NTU method considering it as a whole, since the exact characterization of the heat transfer coefficients in the different regions of the vapour generator was out of the scope of this work.

Hence, the electric power produced by the ORC is equal to:

$$P_{ORC,el} = \dot{m}_f\cdot[\eta_m\cdot\eta_{el}\cdot\Delta h_e - \Delta h_p/(\eta_m\cdot\eta_{el})] \quad (5)$$

where $\dot{m}_f$ is the organic fluid flow rate, η_m the mechanical efficiency, η_{el} the electric efficiency, Δh_e and Δh_p the actual specific enthalpy difference across the expander and the pump. More precisely, the organic working fluid has a flow rate design value of 0.21 kg/s that is adjusted, at every time step, according to an iterative procedure to achieve the fixed overheating temperature difference. In Fig. 3 the ORC electric efficiency by varying the inlet oil temperature is illustrated: the efficiency increases while the oil temperature increases and reaches a maximum value when the oil temperature is above 200 °C in accordance with data from the manufacturer.

With regard to the output thermal power, it is evaluated as in Eq. (6):

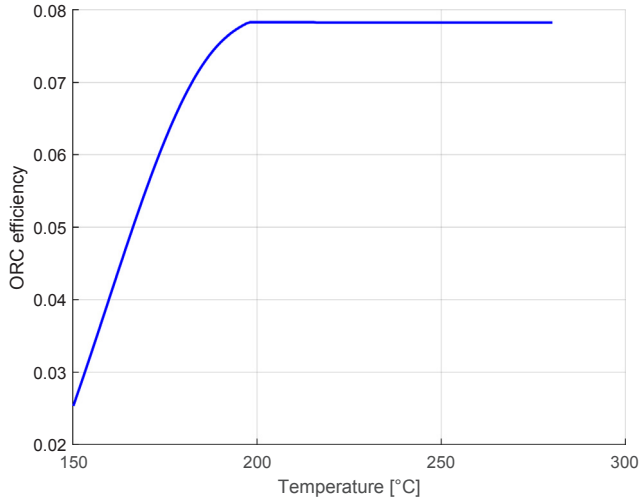

Fig. 3. ORC electric efficiency by varying the inlet oil temperature.

$$P_{ORC,out} = \dot{m}_c \cdot c_{p,c} \cdot (T_{out} - T_{in}) \quad (6)$$

with $\dot{m}_c$ the cooling water flow rate, $c_{p,c}$ the specific heat of the cooling water and T_{out} and T_{in} the outlet and inlet temperatures of the cooling water at the condenser. The cooling water is supposed to be the return water from the final user's heating system with an inlet temperature and mass flow rate at the condenser equal to 60 °C and 0.5 kg/s respectively (assessed by assuming a final user's thermal demand of 18–20 kW, as for the prototype design). Moreover, a minimum temperature difference between the inlet temperature of the cooling water and the condensing temperature of the working fluid has been fixed equal to 12 °C (Fig. 4). As previously mentioned, in this study it has been assumed for simplicity that all the heat produced can be used to cover the thermal demand of a building, without taking into account the interaction with additional boilers.

3.3. Model of the PCM thermal energy storage equipped with heat pipes

The thermal energy storage tank is used to collect the thermal energy produced by the solar field or to supply energy to the ORC when solar energy is scarce. Indeed the ORC needs that the inlet oil temperature at the evaporator is within a certain range to assure a good performance in terms of electric efficiency (see Fig. 3). However, because of the use of reversible heat pipes, the TES cannot be charged and discharged simultaneously.

The PCM storage tank has been modelled according to the guidelines of the IEA Task 32 report on advanced storage concepts [39], where a detailed description of Type 185 is provided. The tank is 1.93 m^3, sized to store 4 h of energy from the solar field. The PCM material is Solar Salt, whose melting temperature is in the range 216–223 °C [40]. The PCM is supposed isotropic and isothermal in each internal time-step (Type 185 uses internal time-steps, shorter than the overall TRNSYS timestep to increase the simulation accuracy [39]). Hysteresis and sub-cooling effects are neglected. The developed model takes into consideration in a simplified way the presence of the heat pipes as heat transfer devices. Indeed they are represented only by means of a limitation in the maximum power exchanged with the oil because of the limited heat pipes capacity (40 kW) and a minimum temperature difference between the oil and the PCM equal to 5 °C. The PCM is represented with a lumped model [39] and its temperature variation due to the heat exchanged with the external heat carrier is given by:

$$\Delta T_{PCM}(t+1) = \Delta T_{PCM}(t) \cdot e^{-[\Delta t_{int-timestep} \cdot k]} \quad (7)$$

where k is a function of both PCM and heat carrier thermal properties [39]. Known the PCM temperature variation, it is possible to assess the heat exchanged as in Eq. (8):

$$Q_{PCM}(t+1) = \int_{t}^{t+1} Q_{PCM}(t) \cdot dt \quad (8)$$

The thermal heat losses of the storage tank towards the environment

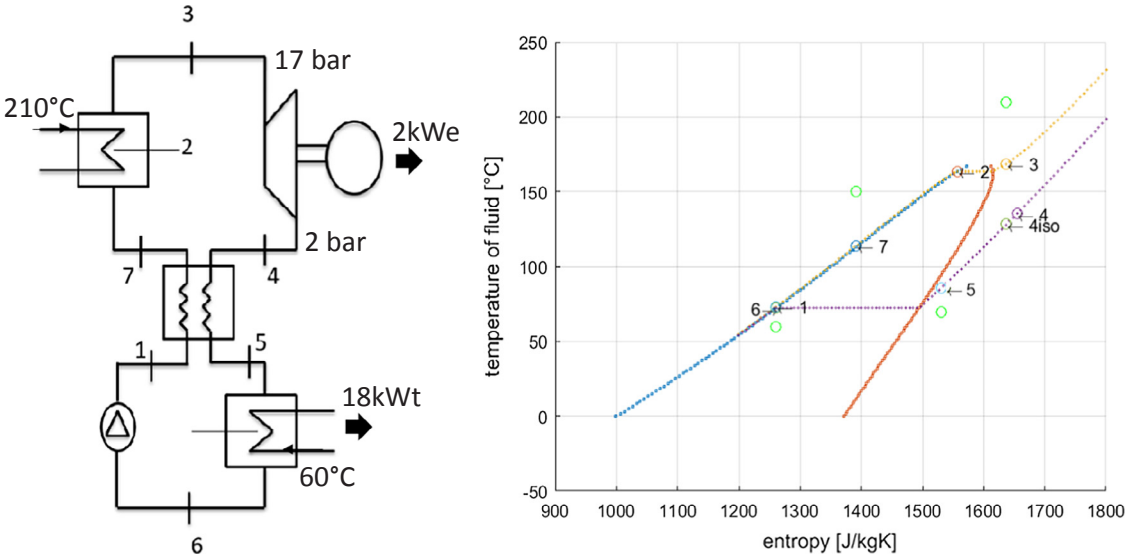

Fig. 4. ORC schematics with design specifications (a) and T-s diagram of the Novec649 at nominal operating conditions (b).

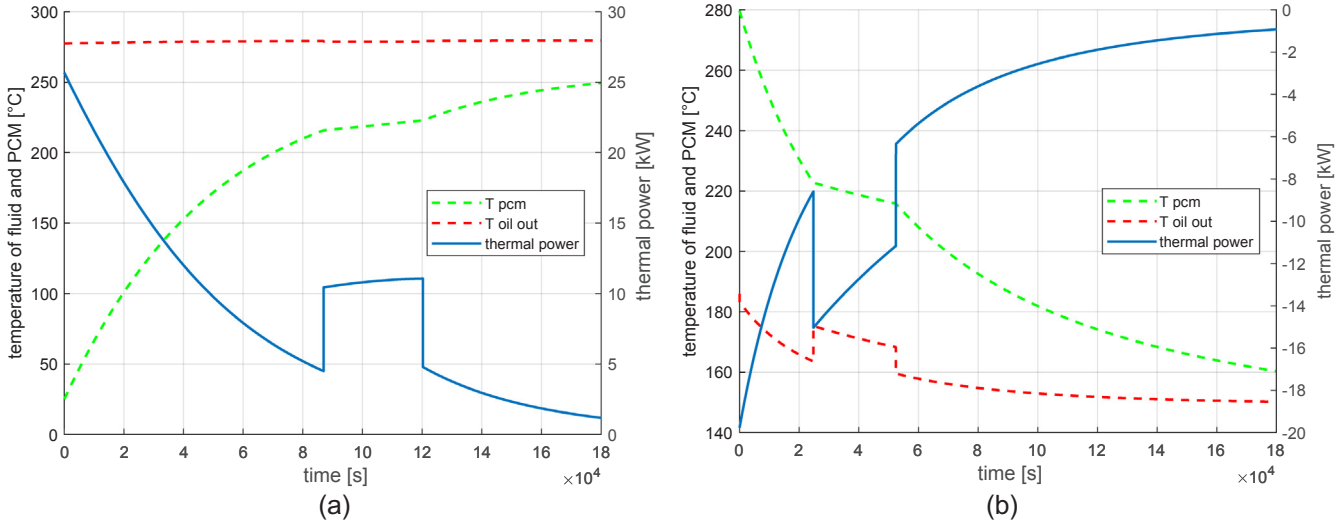

Fig. 5. Charging (a) and discharging (b) phase of the modelled PCM storage system.

are assessed considering a thermal resistance of the storage of 0.4 W/m^2 K. Further details about Type 185 can be found in [39].

In Fig. 5 the obtained behaviour of the PCM storage during charging and discharging processes is illustrated, considering given operating conditions. In particular Fig. 5a shows PCM charging, assuming that heat is provided by oil from the solar field at design condition (oil temperature 280 °C and oil flow rate 3 kg/s). When the process starts, PCM is at ambient temperature. First sensible heat is exchanged and PCM temperature increases up to the melting point in the range 216–223 °C. The charging phase lasts about 4 h as per the design specifications. The thermal power exchanged shows a sharp rise when latent heat is exchanged. Similarly, during the discharging phase (Fig. 5b), PCM is initially at the maximum temperature of 280 °C and heat is removed by oil from the ORC at design conditions (oil temperature 150 °C and oil flow rate 0.22 kg/s). First sensible heat is exchanged and then latent heat when the thermal power shows a sharp decrease, while PCM temperature is almost constant in the melting temperature range.

3.4. Other components

The inertia of the system has been modelled by means of pipes (Type 604), which take into account the inertia of the LFR solar field pipelines, the pipelines for the connection to the TES and the thermal inertia of the ORC unit. They have been sized on the basis of the prototype plant specifications.

In order to implement the control strategy described below, two diverters and two mixers are used to divert the flow of the oil (represented by the 3-way valves in Fig. 1) depending on the operation mode of the plant (see Section 3.5).

3.5. Operation modes

The operation of the integrated system depends on the solar radiation and the state of charge of the TES. At night or during cloudy days, when the DNI is zero or very low, the system is off (OM2). As soon as the DNI achieves a minimum threshold level (100 W/m^2) the main oil pump is switched on. Therefore, the diathermic oil, used to transfer heat from the solar field, flows to the TES or to the ORC depending on its temperature and on the amount of the collected thermal power at the receiver. If the collected thermal power or the oil temperature are low, the oil circulates only towards the TES (OM3) with a flow rate based on current thermal power and TES temperature (the $T_{LFR,out}$ is set 10 °C above the $T_{TES,av}$). Once the collected thermal power reaches a given threshold ($P_{ORC,in}$ > 15 kW), the TES unit is by-passed and the oil is diverted directly to the ORC unit (OM1), in this case the temperature set-point of the oil from the solar field is fixed at 210 °C (nominal temperature of the ORC see Fig. 3), thus the flow rate changes according to the current thermal power available. On the contrary, when the collected thermal power exceeds the request of the ORC unit, the oil flow is split: part flows to the ORC plant and part to the TES to be recovered (OM4). In this operation mode there are two options, one consists of feeding the ORC with oil at 210 °C if the $T_{TES,av}$ is below 200 °C, or, when the latter condition is not verified, the flow rate is adjusted to have the oil temperature 10 °C above the average temperature of the TES (as in OM3). However, if the TES is completely

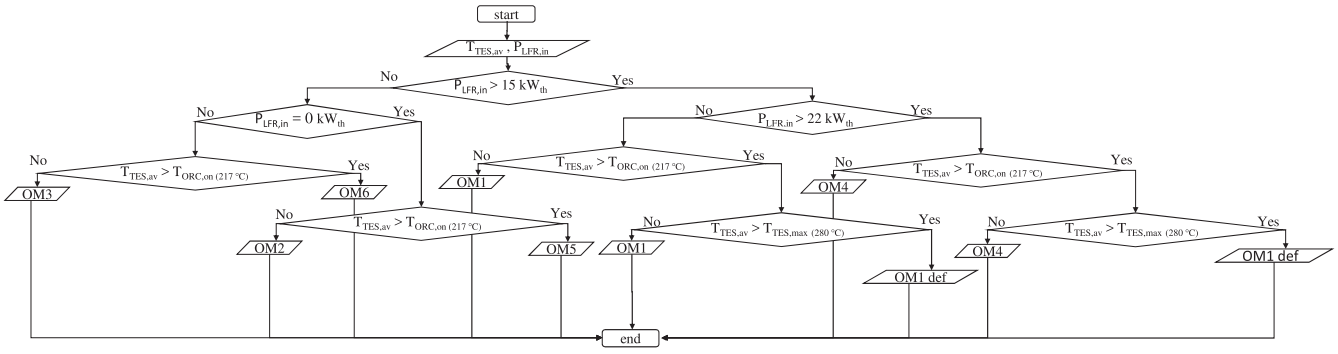

Fig. 6. Flow chart of the control strategy of the plant.

Table 1
Description of the operating conditions for the different operation modes.

Operation mode	Description	Operating conditions
OM1	LFR supplies ORC	T_{oil} = 210 °C
OM2	System off	–
OM3	LFR supplies TES	T_{oil} = $T_{TES,av}$ + 10 °C
OM4	LFR supplies TES and ORC	T_{oil} = 210 °C if $T_{TES,av}$ < 200 °C or $T_{TES,av}$ > 280 °C otherwise T_{oil} = $T_{TES,av}$ + 10 °C if $T_{TES,av}$ > 200 °C
OM5	TES supplies ORC	Oil flow rate 0.22 kg/s
OM6	TES and LFR supply ORC	T_{oil} = 210 °C and oil flow rate 0.22 kg/s

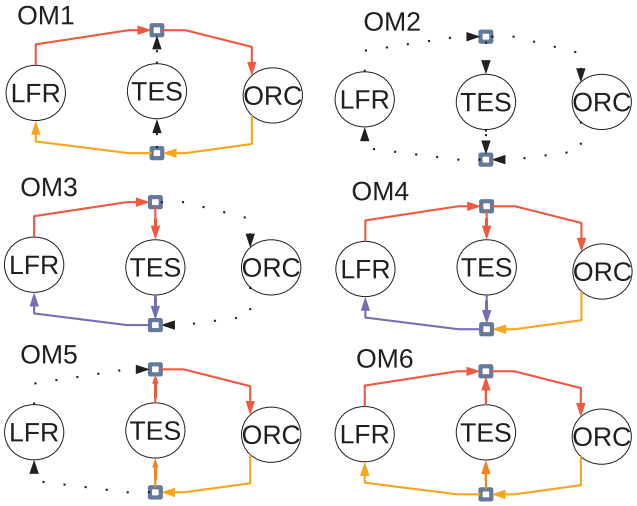

Fig. 7. Scheme of the different operation modes of the prototype plant.

charged ($T_{TES,max}$ is 280 °C), part of the LFRs are defocused and the system runs according to OM1 mode. Because of the design of the LFRs, entire rows are individually defocused in order to achieve the desired output thermal power. Considering the peak output thermal power from the solar field and the number of rows, the output thermal power is adjusted by steps of about 4 kW_t starting from the external rows.

When, instead, not enough power is produced by the solar field and the average TES temperature is within a given range ($T_{ORC,on}$ = 217 °C and $T_{ORC,off}$ = 215 °C), its thermal energy can be used to run the ORC unit as follows. When the collected thermal energy at the receiver is lower than the nominal input power at the ORC unit (i.e. 22 kW), the oil flow rate from the solar field is mixed with that from the TES in order to maintain the oil temperature at 210 °C and the nominal oil flow rate to the ORC of 0.22 kg/s (OM6). In case the solar field is off, oil from the TES only flows to the evaporator of the ORC (at the ORC nominal flow rate of 0.22 kg/s) thus assuring its operation for a maximum of 4 h (OM5). In this way, it is possible to extend the operation of the system by collecting the surplus thermal power from the solar field during the day and discharging it when there is no sun.

Set-points and threshold values to switch from an operation mode to another have been chosen according to the design and operational specifications of the different subsystems. Fig. 6 shows the control logic flow chart. Table 1 summarizes the operating conditions for every operation mode, while Fig. 7 reports the scheme of the different operation modes of the prototype plant.

Table 2
Monthly average overall efficiency of the plant and of its main components.

	Eff_{LFR}	Eff_{TES}	$Eff_{ORC,el}$	$Eff_{ORC,th}$	Heat losses	Eff_{TOT}	h_{ORC}
January	26.2%	81.1%	6.2%	79.8%	48.3%	16.8%	121.7
February	30.8%	66.0%	6.2%	80.5%	43.4%	18.7%	125.0
March	41.5%	73.0%	6.5%	81.6%	25.6%	25.5%	244.8
April	46.8%	84.9%	6.4%	82.0%	21.6%	28.2%	296.5
May	50.1%	77.4%	6.6%	82.0%	18.4%	30.4%	357.0
June	53.0%	87.7%	6.6%	82.4%	14.9%	29.9%	426.3
July	52.1%	91.4%	6.6%	82.1%	16.0%	31.8%	434.0
August	49.4%	81.1%	6.5%	82.1%	16.9%	29.7%	387.5
September	45.9%	83.2%	6.6%	81.8%	20.3%	29.1%	315.2
October	36.5%	79.1%	6.5%	81.2%	31.2%	23.2%	191.3
November	30.9%	59.9%	6.5%	80.0%	42.2%	19.8%	132.7
December	23.8%	17.0%	6.2%	78.9%	54.7%	14.8%	104.5

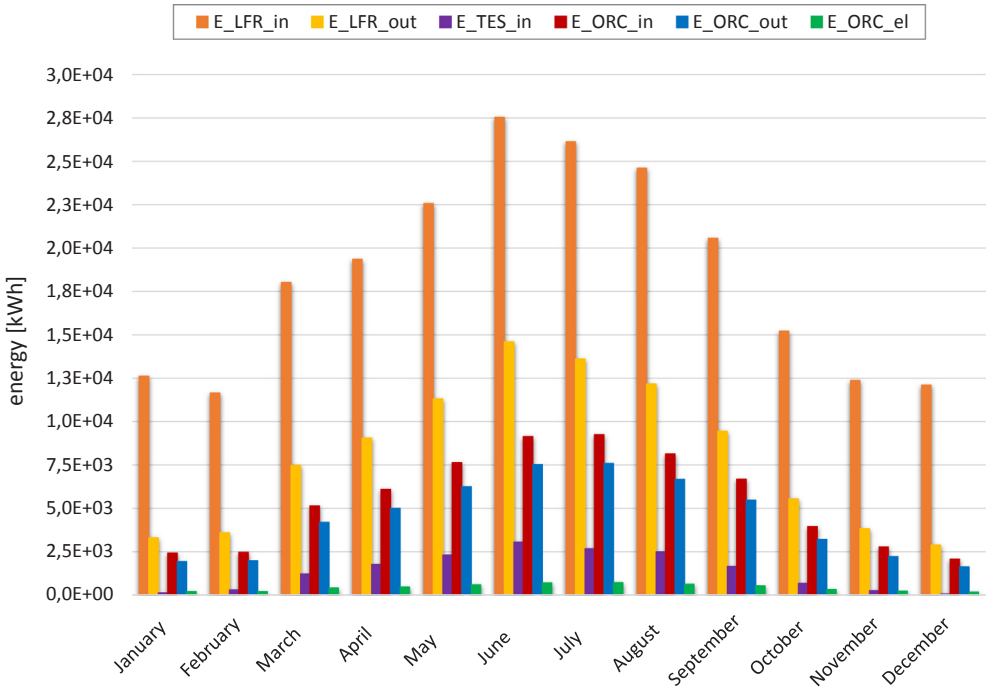

Fig. 8. Monthly energy balance for the solar ORC plant.

4. Results and discussion

In this section the simulation results for the small-scale solar concentrator ORC plant are presented. Weather data (i.e. solar radiation and ambient temperature) have been taken from Meteonorm database on an hourly basis for the city of Cagliari in Italy (local coordinates 39° 22′ 38.41″ N and 9° 12′ 16.61″ E). Cagliari has been selected because it is a representative geographic location for solar heat and power system. Indeed a good solar radiation is available throughout the year, allowing a good performance of the system. The plant has been assumed along the North-South direction. The used simulation time step is 10 min.

For the scope of this analysis, the plant is supposed to operate at its nominal operating conditions whenever possible. The monthly overall energy balance of the system is shown in Fig. 8. As expected, the input and output solar energy of the LFR solar field are much higher during summer and spring because of the higher DNI and hours of radiation. Despite the solar multiple of the plant, the surplus heat is limited. Most of the energy from the solar field indeed is used to supply the ORC unit and only a reduced amount flows into the TES. Although low, the electric energy production by the ORC is significantly affected by the variable solar radiation during the year.

Plant performance have been evaluated also in terms of monthly conversion efficiencies of the different subsystems as reported in Table 2. The solar field efficiency (Eff_{LFR}) is the ratio between the input solar energy and the output energy from the solar collector to the ORC unit and/or the TES, according to the operation mode. Because of the solar angles, which considerably affect the values of the IAM and the cosine effect, the solar field efficiency varies largely throughout the year. More precisely, it ranges from almost 24% in December to 53% in June with an annual average value of about 40.6% which represents a satisfactory target. The thermal energy storage efficiency (Eff_{TES}) is the ratio between the outlet thermal energy towards the ORC (discharging) and the inlet thermal energy from the LFR solar field (charging). On the basis of the control logic defined in the model (see Section 3.5), OM5 and OM6 modes start when the TES temperature reaches 217 °C and stop as soon as the temperature is 215 °C. In this way, the discharging of the TES is able to exploit the higher heat transfer coefficient due to the phase change of the storage mean. On the other hand, the reduced discharging temperature range limits the annual operating hours of the system in OM5 and OM6 (see Table 3). Moreover, this entails also low TES efficiencies during cold season (with the exception of January because the TES initial temperature has been set at 200 °C). In winter, indeed, the DNI is usually not enough to supply adequate thermal power to the TES for its melting and the surplus energy from the solar field cannot be used during night time for most of the days. However, in the real operation of the system this amount of thermal energy could be directly supplied to the final user for heating purposes thus significantly increasing the efficiency of the TES also in winter time.

With regard to the ORC, its electric efficiency ($Eff_{ORC,el}$), i.e. the ratio between the output electric energy and the inlet thermal energy to the ORC, remains almost constant throughout the year and above 6.2%, similarly to values shown in [16]. On the contrary, the thermal efficiency of the ORC ($Eff_{ORC,th}$), defined as the ratio between the output and the inlet thermal energy of the ORC, is close to 80% reaching the peak value of 82.4% in June. Given the high solar radiation in summer and the corresponding collected thermal power from the LFR, the system shows a very interesting potential also as trigeneration plant. However, because of the further increase of its complexity and the reduction of its electric efficiency in case of solar cooling applications in summer, this configuration has not been investigated for the moment.

As far as the total conversion efficiency of the plant (Eff_{TOT}) is concerned, namely the ratio between the output electric and thermal energy and the inlet solar energy, it varies because of the different solar field efficiency during the year and it ranges from 14.8% in December to almost 32% in summer. As reported in Section 3.4, the model takes into account also the heat losses in the pipelines and in the main components, which globally account for more than 20% of the available output thermal power from the LFR. In December, the thermal losses in the TES account for about 54% of the LFR thermal power. This is mainly due to: (i) the impossibility of supplying the ORC with TES energy because the TES temperature is below the melting point most of the time in winter, thus stored energy is not used; and to (ii) the reduced DNI in winter, which does not allow to run the ORC unit in OM1 and OM4 for long periods. Furthermore, the operating hours of the system in OM3 (TES charging) are more than 40% higher in winter than in summer.

In terms of operating hours, the ORC unit is able to work more than 3100 h. Moreover the operating hours of the ORC unit could be sensibly increased by varying the set-point temperatures of the TES in OM5 and OM6, i.e. when the TES supplies the ORC. However, this would reduce the electric efficiency of the ORC and the overall energy production [41].

As far as the energy production is concerned, in the present configuration the ORC unit is able to generate about 5110 kWh_e/year and 53,670 kWh_t/year, which represent a considerable amount of energy for household applications. Indeed, compared to the results presented by Calise et al. [29] for a 6 kWe solar-ORC set in an Italian location with a similar latitude, the proposed prototype plant can produce 30% more

Table 3
ORC performance data: average thermal input power, average electric and thermal output power and average efficiency during each month for the different operation modes.

		January	February	March	April	May	June	July	August	September	October	November	December	Working hours
OM1	$P_{ORC,in}$ [kW]	9.7	9.6	13.7	11.5	14.7	15.5	13.5	13.3	13.8	12.6	11.5	9.5	347 h
	$P_{ORC,out}$ [kW]	7.7	7.7	10.9	9.2	11.8	12.4	10.7	10.7	11.0	10.1	9.1	7.6	
	$P_{ORC,el}$ [kW]	0.8	0.8	1.1	0.9	1.2	1.2	1.1	1.1	1.1	1.0	0.9	0.8	
	$Eff_{ORC,el}$ [%]	3.6	3.8	5.3	4.4	5.8	5.7	5.0	5.3	5.2	4.9	4.2	3.8	
OM4	$P_{ORC,in}$ [kW]	23.4	23.4	24.2	24.1	24.5	24.6	24.5	24.4	24.5	23.9	23.4	22.7	1998 h
	$P_{ORC,out}$ [kW]	18.6	18.8	19.9	20.0	20.2	20.5	20.3	20.2	20.2	19.5	18.8	17.9	
	$P_{ORC,el}$ [kW]	1.9	1.9	2.1	2.1	2.1	2.1	2.1	2.1	2.1	2.0	1.9	1.8	
	$Eff_{ORC,el}$ [%]	7.2	7.2	7.6	7.6	7.7	7.7	7.7	7.7	7.6	7.4	7.2	7.0	
OM5	$P_{ORC,in}$ [kW]	15.9	15.7	15.8	15.9	15.9	15.9	15.9	16.0	15.9	15.7	15.4	0.0	621 h
	$P_{ORC,out}$ [kW]	12.8	12.6	12.7	12.8	12.8	12.8	12.8	12.8	12.8	12.6	12.5	0.0	
	$P_{ORC,el}$ [kW]	0.7	0.6	0.6	0.7	0.7	0.7	0.7	0.7	0.7	0.6	0.6	0.0	
	$Eff_{ORC,el}$ [%]	4.1	3.8	4.0	4.1	4.1	4.2	4.2	4.2	4.1	3.9	3.6	0.0	
OM6	$P_{ORC,in}$ [kW]	20.3	20.6	19.2	18.4	18.8	18.2	18.6	19.2	18.7	19.5	18.4	0.0	171 h
	$P_{ORC,out}$ [kW]	15.9	16.3	15.2	14.5	14.9	14.4	14.7	15.2	14.7	15.3	14.5	0.0	
	$P_{ORC,el}$ [kW]	1.5	1.5	1.3	1.2	1.2	1.1	1.2	1.3	1.2	1.3	1.2	0.0	
	$Eff_{ORC,el}$ [%]	6.9	6.7	6.5	6.1	5.9	5.6	5.9	6.2	6.1	6.4	6.0	0.0	

thermal energy and 18% more electric energy, despite the lower size of the ORC unit.

The main purpose of this analysis is to evaluate how the ORC electric efficiency varies during plant operation and how it is affected by the operation modes of the implemented control strategy (see the operation modes in Section 3.5). Therefore, the ORC performance data are evaluated on a monthly basis considering the operation modes OM1, OM4, OM5 and OM6, i.e. when the ORC is on. In general, the ORC unit achieves the highest electric efficiency in mode OM4, when the solar power is so high to supply not only the ORC, but even the TES. More precisely, the $Eff_{ORC,el}$ reaches the monthly average peak value of 7.75% in June. In mode OM4 the annual average output electric power is higher than 2.0 kW, which is very close to the design value. Moreover, this condition occurs for almost 2000 h/year. Because of the set-point temperatures of the TES, the ORC is able to achieve high conversion efficiencies also in mode OM6, when both the LFR and TES supply power to the ORC. However, this operating mode is limited to about 170 h/year. Since high DNI and hours of radiation are needed to melt the PCM in the TES, OM6 and OM5 do not occur in December and in general such operation modes are mainly present in summer season. Finally, because of the limited input thermal power and the intermittent operation of the system in mode OM1, the ORC unit achieves an annual average output power and electric conversion efficiency of about 1 kWe and 4.8% in this state. Indeed, in winter the DNI is low and no sufficient power is collected by the solar field, while in summer this operation mode occurs in between the other operating modes. Therefore, the annual hours of operation in mode OM1 are limited to less than 350 h. Despite the defocusing of the solar plant is foreseen by the model (OM1 defocused see Fig. 6) such condition does not occur during the simulated year for the city of Cagliari.

Table 3 reports the monthly average thermal input power, electric and thermal output power and efficiency of the ORC system during operation modes OM1, OM4, OM5 and OM6.

Regarding operation mode OM3, i.e. when the solar field has not enough power to run the ORC and it supplies only the TES, the annual operating hours of the plant are almost 1250. Finally, the plant remains off (OM2) for about 4384 h in a year (i.e. more than half of the annual hours).

In order to better appreciate how the plant switches from an operation mode to another, plant performance has been analysed also on an hourly basis. In particular, the power trends and the sequence of operation modes are evaluated for typical working days representative of the 4 seasons: the fourth day of February, April, August and October have been considered for the purpose. Fig. 9a–d show the daily trend of LFR input and output power, ORC input thermal power and output electric power, during the different operation modes.

This investigation has confirmed that mode OM4 runs often for long periods: indeed also in winter the solar radiation can be sufficiently high, thus the solar field supplies both the ORC and the TES as reported in Fig. 9a. When the power from the LFR is not enough, the LFR supplies only the ORC (OM1) or only the TES in case of reduced temperatures/power (OM3). Instead, in Fig. 9b the solar radiation in spring is variable during the day and it is not so high, with a maximum input power lower than 90 kW. This leads to a different schedule of the operation modes: first only the TES is supplied (OM3), then the radiation increases and both the TES and the ORC are supplied (OM4), finally it

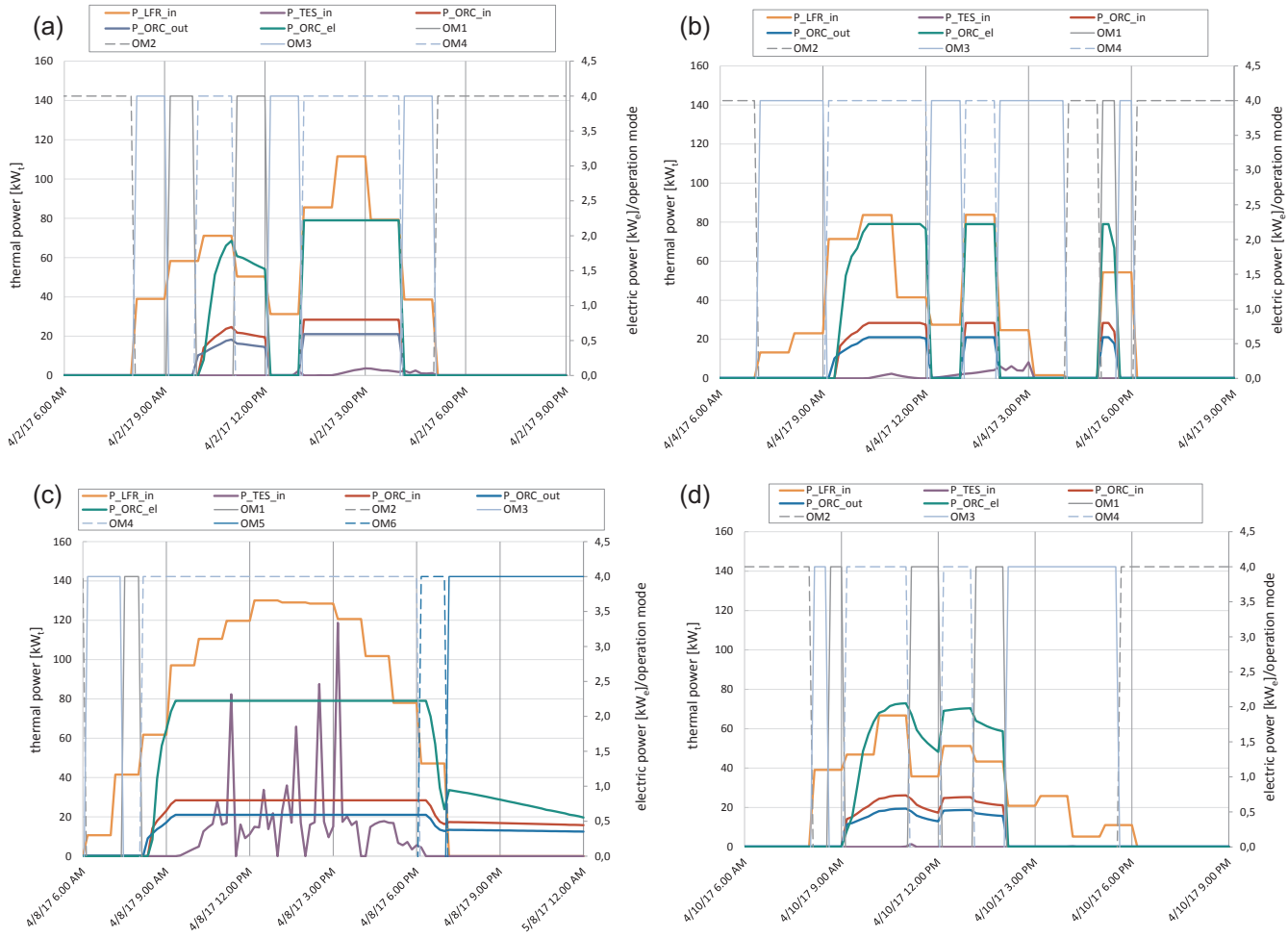

Fig. 9. (a–d) daily trend of plant performance and operation modes for typical working days in (a) winter, (b) spring, (c) summer, (d) autumn.

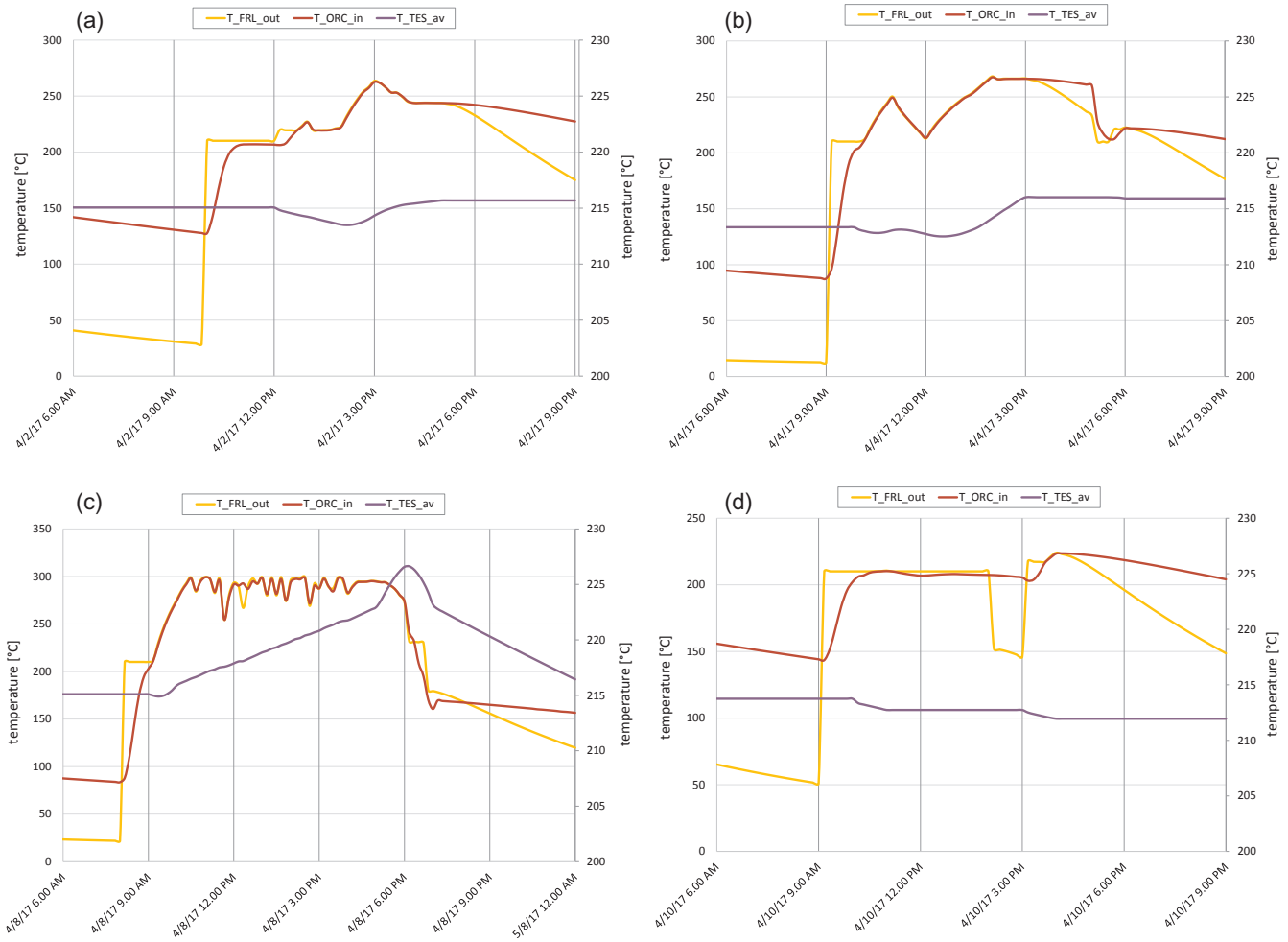

Fig. 10. (a–d) daily trend of temperatures in (a) winter, (b) spring, (c) summer, (d) autumn.

decreases again and only the ORC is supplied (OM1). During the considered summer day (Fig. 9c), the energy stored in the TES is discharged to the ORC to integrate the energy from the LFR (OM6) or alone (OM5) at night hours. It can be seen that during OM5 the TES cannot supply the ORC at nominal conditions, because its temperature is too low, the electric power produced is limited and it decreases while the TES discharges its energy. In autumn the solar radiation for the considered typical day is even lower than in spring and the system starts to supply first the TES (OM3) and then, when the solar power increases, also the ORC without (OM1) and with (OM4) the having a surplus energy to be stored in the tank (Fig. 9d).

Finally, Fig. 10a–d report the daily trend of temperatures at the outlet of the LFR solar field, at the inlet of the ORC unit, i.e. the inlet oil temperature at the evaporator, and the average temperature of the PCM storage tank. Results show that in winter the collected thermal power allows to supply the ORC unit and to start the melting of the PCM material, however the upper bound of 217 °C to activate the OM5 phase is not reached, as previously discussed. Also in spring, despite the varying DNI and the corresponding temperature at the LFR, the collected thermal power is enough just to start the melting of the PCM. On the contrary, in summer when the collected thermal power is higher, the temperature of the PCM is well above the melting temperature range during the day, thus allowing the operation of the system in modes OM5 and OM6 depending on the DNI. Finally, in autumn the trend is very similar to the considered spring day, although the maximum temperature at the LFR outlet and ORC inlet are lower. Fig. 10a–d highlight also the thermal inertia of the system. At the plant start up in the morning, the control strategy forces the LFR outlet temperature at 210 °C according to OM1, but it takes some time before the ORC inlet temperature increases as well. The same effect can be observed also in late afternoon or sunset. The residence time of the oil in the pipes and its thermal inertia are responsible for the heat losses discussed previously and reported in Table 2.

Eventually, a first economic assessment of the considered system is presented. The analysis is based on the prototype plant costs and it is aimed at highlighting the present necessary investment, comparing it with available data in literature for other systems, and at identifying possible improvements to be achieved as results of the EU project [30].The investment cost of the prototype plant has been estimated around 150′000€. This means a specific overall cost of 75000€/kWe, which is significantly higher than the investment cost of the other plants reported in literature [26,29]. In particular, the 50kWe PTC-ORC plant proposed by Patil et al. [26] has a specific capital cost of about 5884.6 USD/kWe, while the 6 kWe solar-ORC prototype plant designed and investigated by Calise et al. [29] has a cost of about 11,407 €/kWe. However, it is important to underline that the other systems have a bigger size than the system here investigated and this aspect helps their economic feasibility. In particular the item that weights more on the overall prototype plant investment is the cost for the innovative TES system equipped with reversible heat pipes. Its cost should be halved thanks to the further design optimization carried on in Innova Micro-solar project [30]. Indeed, purpose of this EU project is to further improve, from a techno-economic point of view, the components of the plant in order to have a feasible product for the large market of solar heat and power generation for domestic and 2 kWe application.

Moreover, based on the energy productivity of the Innova

MicroSolar system obtained from the simulation results, an economic analysis in terms of LCOE has been carried out. The present value of the total investment cost is equal to the sum of the capital expenditure (CAPEX) and the present value of the operating expenditure (OPEX) where the OPEX incurred at the i-th year is assessed as in Eq. (9):

$$OPEX(i) = 0.02 \cdot CAPEX \cdot (1 + ir)^{i-1} \quad (9)$$

where ir is the inflation rate assumed equal to 5% per annum and i the year of operation in the range 1 to 25 which corresponds to the lifetime of the plant [26]. The present value of the OPEX is determined using a discount rate (dr) of 12% according to Eq. (10):

$$OPEX = \sum_{i=1}^{lifetime} \frac{OPEX(i)}{(1 + dr)^i} \quad (10)$$

Finally, also the total electric energy generated over the lifetime of the plant needs to be reported in its present economic value (Eq. (11)):

$$E_{gen,tot} = \sum_{i=1}^{lifetime} \frac{E_{gen}(i)}{(1 + dr)^i} \quad (11)$$

where $E_{gen}(i)$ is the electric energy generated in the i-th year.

Hence, the LCOE is calculated as the ratio of the present value of the total investment over the plant lifetime and the present value of the total energy generated during its operation [26], as in Eq. (12):

$$LCOE = \frac{\text{present value of the total investment over plant life } [€]}{\text{present value of the total energy generated over plant life } [\text{kWh}]} = \frac{CAPEX + OPEX}{E_{gen,tot}} \quad (12)$$

Considering an annual electric energy production of the Innova MicroSolar plant of about 5100 kWh_e for the city of Cagliari, a LCOE of 4.6 €/kWh is obtained. Because of the reduced size of the ORC unit and the high investment cost, the LCOE of the prototype is extremely high compared with other values in literature. For example, the economic results of Patil et al. [26] showed a LCOE of their 50 kWe PTC-ORC of about 0.26 USD/kWh for the city of Ahmedabad in India.

However, the Innova MicroSolar prototype plant generates also a large amount of thermal energy which corresponds to about 53,670 kWh/year. A simple payback period (PBP) can be assessed by dividing the investment cost of the plant by the achievable energy savings (i.e. energy not purchased from the electricity grid with a price of 0.21 €/kWh [42] or from the gas grid with a price of 0.07 €/kWh [43]). Assuming for simplicity that all the electric and thermal energy can be used directly by the final user, a PBP of about 30 years is calculated for the prototype. It implies that for achieving a PBP lower than 10 years, the plant cost has to be reduced to one third of the present cost or the production should be improved to increase the achievable savings. Even Calise et al. [29] for their 6 kWe ORC coupled with evacuated flat-plate solar collectors showed a PBP of about 10 years, thanks also to the higher price of the natural gas considered and to the exploitation of a feed in tariff incentive scheme. The proposed economic analysis is uniquely aimed at providing an idea of the feasibility of the considered system, it does not take into account the foreseen improvements of the components and it is affected by several simplifications and lack of information at this stage. However it is helpful to highlight critical issues and barriers to overcome for the uptake of this new technology.

5. Conclusions

In this work, the overall performance of an innovative integrated system consisting of a concentrated linear Fresnel reflectors solar field, a 2 kWe ORC unit coupled with a phase change material storage tank equipped with heat pipes has been investigated by means of a simulation analysis in TRNSYS. Ad hoc subroutines for the different subsystems have been developed by the authors in order to better include the peculiarities of each system with respect to its actual design. The simulation analysis carried out has provided useful information for the forthcoming assembly and testing of the real prototype plant. Indeed, according to the varying ambient conditions, the influence of the different operation modes of the prototype plant have been evaluated in terms of overall plant efficiency and power production, conversion efficiency of its main components, operating hours and working temperatures.

Main findings are summarized below:

- As expected, the overall conversion efficiency and the corresponding related power generation are considerably affected by ambient conditions and incident DNI. Therefore, the higher production is achieved in summer with a peak overall conversion efficiency of about 31.8%. The electric efficiency of the organic Rankine cycle unit is almost constant throughout the year with a monthly average value higher than 6.2%. However, more than 70% of the annual operating hours of the ORC unit occur in the hot season in the period April-September with a peak monthly operation of more than 430 h in June. The annual operating hours of the ORC unit are more than 3100 h with an annual electric and thermal energy production of about 5100 kWh_e and 53,670 kWh_t respectively, which represent a considerable amount of energy for households.
- In terms of conversion efficiency and electric power production the system proved to have the best performance in mode OM4, i.e. when the collected thermal power from the solar field is high and it supplies bot the Rankine cycle and the storage tank.
- High performance is achieved also in modes OM6, i.e. when the storage supplies the organic Rankine cycle plant together with the solar field. However, because of the set-point temperatures of the storage tank, the operating hours of the system are limited to 170 h/year in OM6.
- Operation modes OM1 (i.e. the solar field supplies directly the organic Rankine cycle unit and the storage tank is by-passed) and OM5 (only the storage supplies the organic Rankine cycle) allow to achieve low electric conversion efficiency because of the limited input thermal power in the organic Rankine cycle unit and of intermittent operation of the system in such conditions.
- The integrated system has shown also a considerable amount of heat losses, which could be sensibly reduced by varying the storage operating temperature set- points or the control strategy of the plant. In winter, indeed, when the collected solar thermal power is not enough to melt the phase change material in the tank, the stored thermal power is then progressively lost to the ambient. This is a critical issue, because it is necessary to find the right trade-off between reducing thermal losses and increasing electric efficiency of the organic Rankine cycle when it is supplied directly from the storage. A solution could be to provide the low temperature heat not used directly to the final user for heating purposes, thus the heat losses of the system could be reduced and the energy storage efficiency not jeopardized.
- Finally, the performance of the system have been evaluated also from an economic point of view in terms of levelized cost of electricity. Because of the reduced size of the plant and its high investment cost, the levelized cost of electricity is about 4.6 €/kWh which is extremely high especially if compared to other technologies. Especially the energy storage system is a critical item to diminish the investment cost. However, purpose of the Innova MicroSolar project is to improve, from a techno-economic point of view, the components of the plant in order to reduce the gap of these innovative systems with other commercial technologies, allowing the economic feasibility of the plant.

Concluding, this work has given some insights into the influence of the design specifications and of the control strategy on the system performance. Therefore, the analysis could serve in the future as a general guide to understand the mutual interactions of the different

subsystems in similar small-scale concentrated solar organic Rankine cycle plants and, consequently, to choose the best operating conditions to improve the achievable production and overall efficiency.

Acknowledgements

This study is a part of the Innova MicroSolar Project, funded in the framework of the European Union's Horizon 2020 Research and Innovation Programme (grant agreement No 723596).

References

[1] United Nations/Framework Convention on Climate Change. Paris Agreement. 21st Conf Parties 2015:3. doi: FCCC/CP/2015/L.9.
[2] IPCC. Renewable Energy Sources and Climate Change Mitigation. 2012. doi: 10.5860/CHOICE.49-6309.
[3] International Energy Agency. Tracking Clean Energy Progress. Energy technology perspectives 2016 excerpt IEA input to the clean energy ministerial. Technology 2016;2016:1–82. http://dx.doi.org/10.1787/energy_tech-2014-en.
[4] Siva Reddy V, Kaushik SC, Ranjan KR, Tyagi SK. State-of-the-art of solar thermal power plants—a review. Renew Sustain Energy Rev 2013;27:258–73. http://dx.doi.org/10.1016/j.rser.2013.06.037.
[5] Kumar V, Shrivastava RL, Untawale SP. Fresnel lens: a promising alternative of reflectors in concentrated solar power. Renew Sustain Energy Rev 2015;44:376–90. http://dx.doi.org/10.1016/j.rser.2014.12.006.
[6] Abbas R, Muñoz J, Martínez-Val JM. Steady-state thermal analysis of an innovative receiver for linear Fresnel reflectors. Appl Energy 2012;92:503–15. http://dx.doi.org/10.1016/j.apenergy.2011.11.070.
[7] Petrollese M, Cocco D. Optimal design of a hybrid CSP-PV plant for achieving the full dispatchability of solar energy power plants. Sol Energy 2016;137:477–89. http://dx.doi.org/10.1016/j.solener.2016.08.027.
[8] Elianto S.R.L – Home n.d. < http://www.eliantocsp.it/index.php/en/ > [accessed November 14, 2017].
[9] Chemisana D, Rosell JI, Riverola A, Lamnatou C. Experimental performance of a Fresnel-transmission PVT concentrator for building-façade integration. Renew Energy 2016;85:564–72. http://dx.doi.org/10.1016/j.renene.2015.07.009.
[10] Tian Z, Perers B, Furbo S, Fan J. Annual measured and simulated thermal performance analysis of a hybrid solar district heating plant with flat plate collectors and parabolic trough collectors in series. Appl Energy 2017;205:417–27. http://dx.doi.org/10.1016/j.apenergy.2017.07.139.
[11] Aboelwafa O, Fateen SEK, Soliman A, Ismail IM. A review on solar Rankine cycles: working fluids, applications and cycle modifications. Renew Sustain Energy Rev 2018;82:868–85.
[12] Tchanche BF, Lambrinos G, Frangoudakis A, Papadakis G. Low-grade heat conversion into power using organic Rankine cycles – a review of various applications. Renew Sustain Energy Rev 2011;15:3963–79. http://dx.doi.org/10.1016/j.rser.2011.07.024.
[13] Quoilin S, Van Den Broek M, Declaye S, Dewallef P, Lemort V. Techno-economic survey of organic rankine cycle (ORC) systems. Renew Sustain Energy Rev 2013;22:168–86. http://dx.doi.org/10.1016/j.rser.2013.01.028.
[14] Ziviani D, Beyene A, Venturini M. Advances and challenges in ORC systems modeling for low grade thermal energy recovery. Appl Energy 2014;121:79–95. http://dx.doi.org/10.1016/j.apenergy.2014.01.074.
[15] Bouvier JL, Michaux G, Salagnac P, Kientz T, Rochier D. Experimental study of a micro combined heat and power system with a solar parabolic trough collector coupled to a steam Rankine cycle expander. Sol Energy 2016;134:180–92. http://dx.doi.org/10.1016/j.solener.2016.04.028.
[16] Taccani R, Obi JB, De Lucia M, Micheli D, Toniato G. Development and experimental characterization of a small scale solar powered organic Rankine cycle (ORC). Energy Procedia 2016;101:504–11. http://dx.doi.org/10.1016/j.egypro.2016.11.064.
[17] Xu G, Song G, Zhu X, Gao W, Li H, Quan Y. Performance evaluation of a direct vapor generation supercritical ORC system driven by linear Fresnel reflector solar concentrator. Appl Therm Eng 2015;80:196–204. http://dx.doi.org/10.1016/j.applthermaleng.2014.12.071.
[18] Antonelli M, Baccioli A, Francesconi M, Desideri U. Dynamic modelling of a low-concentration solar power plant: a control strategy to improve flexibility. Renew Energy 2016;95:574–85. http://dx.doi.org/10.1016/j.renene.2016.04.053.
[19] Freeman J, Hellgardt K, Markides CN. Working fluid selection and electrical performance optimisation of a domestic solar-ORC combined heat and power system for year-round operation in the UK. Appl Energy 2017;186:291–303. http://dx.doi.org/10.1016/j.apenergy.2016.04.041.
[20] Shuai Li, Hongjie Ma, Li W. Dynamic performance analysis of a solar organic Rankine cycle with thermal energy storage. Appl Therm Eng 2018;129:155–64.
[21] He Y-L, Mei D-H, Tao W-Q, Yang W-W, Liu H-L. Simulation of the parabolic trough solar energy generation system with Organic Rankine Cycle. Appl Energy 2012;97:630–41. http://dx.doi.org/10.1016/j.apenergy.2012.02.047.
[22] Freeman J, Guarracino I, Kalogirou SA, Markides CN. A small-scale solar organic Rankine cycle combined heat and power system with integrated thermal energy storage. Appl Therm Eng 2017;127:1543–54. http://dx.doi.org/10.1016/j.applthermaleng.2017.07.163.
[23] Manfrida G, Secchi R, Stańczyk K. Modelling and simulation of phase change material latent heat storages applied to a solar-powered Organic Rankine Cycle. Appl Energy 2016;179:378–88. http://dx.doi.org/10.1016/j.apenergy.2016.06.135.
[24] Quoilin S, Aumann R, Grill A, Schuster A, Lemort V, Spliethoff H. Dynamic modeling and optimal control strategy of waste heat recovery Organic Rankine Cycles. Appl Energy 2011;88:2183–90. http://dx.doi.org/10.1016/j.apenergy.2011.01.015.
[25] Hernandez A, Desideri A, Gusev S, Ionescu CM, Den Broek MV, Quoilin S, et al. Design and experimental validation of an adaptive control law to maximize the power generation of a small-scale waste heat recovery system. Appl Energy 2017;203. doi: 10.1016/j.apenergy.2017.06.069.
[26] Patil VR, Biradar VI, Shreyas R, Garg P, Orosz MS, Thirumalai NC. Techno-economic comparison of solar organic Rankine cycle (ORC) and photovoltaic (PV) systems with energy storage. Renew Energy 2017;113:1250–60. http://dx.doi.org/10.1016/j.renene.2017.06.107.
[27] Barbieri ES, Spina PR, Venturini M. Analysis of innovative micro-CHP systems to meet household energy demands. Appl Energy 2012;97:723–33. http://dx.doi.org/10.1016/j.apenergy.2011.11.081.
[28] Bianchi M, De Pascale A, Melino F. Performance analysis of an integrated CHP system with thermal and Electric Energy Storage for residential application. Appl Energy 2013;112:928–38. http://dx.doi.org/10.1016/j.apenergy.2013.01.088.
[29] Calise F, d'Accadia MD, Vicidomini M, Scarpellino M. Design and simulation of a prototype of a small-scale solar CHP system based on evacuated flat-plate solar collectors and Organic Rankine Cycle. Energy Convers Manage 2015;90:347–63. http://dx.doi.org/10.1016/j.enconman.2014.11.014.
[30] Innova-Microsolar n.d. < http://innova-microsolar.eu/ > [accessed November 3, 2017].
[31] Enogia | Home n.d. < http://www.enogia.com/ > [accessed November 14, 2017].
[32] 3M™ Novec™ 649 Engineered Fluid n.d.
[33] Northumbria University | Newcastle upon Tyne | Study in the Best Student City n.d. < https://www.northumbria.ac.uk/ > [accessed December 28, 2017].
[34] Thermacore n.d. < http://www.thermacore-europe.com/ > [accessed December 28, 2017].
[35] S.TRA.TE.G.I.E. srl n.d. < http://www.strategiesrl.com/eng/Default.aspx > [accessed December 29, 2017].
[36] Welcome|TRNSYS : Transient System Simulation Tool n.d. < http://www.trnsys.com/ > [accessed November 14, 2017].
[37] MATLAB – MathWorks n.d. < https://www.mathworks.com/products/matlab.html > [accessed November 14, 2017].
[38] Burkholder F, Kutscher C. Heat-Loss Testing of Solel's UVAC3 Parabolic Trough Receiver 2008.
[39] Gantenbein P, Jaenig D, Kerskes H, Van Essen M. Final report of Subtask B " Chemical and Sorption Storage " The overview A Report of IEA Solar Heating and Cooling programme -Task 32 Advanced storage concepts for solar and low energy buildings Report B7 of Subtask B 2008.
[40] Serrano-López R, Fradera J, Cuesta-López S. Molten salts database for energy applications. Chem Eng Process 2013. http://dx.doi.org/10.1016/j.cep.2013.07.008.
[41] Cioccolanti L, Tascioni R, Arteconi A. Simulation analysis of an innovative micro-solar 2kWe Organic Rankine Cycle plant for residential applications. Energy Procedia 2017;142. http://dx.doi.org/10.1016/j.egypro.2017.12.541.
[42] Electricity price statistics – Statistics Explained n.d. < http://ec.europa.eu/eurostat/statistics-explained/index.php/Electricity_price_statistics > [accessed March 5, 2018].
[43] Natural gas price statistics – Statistics Explained n.d. < http://ec.europa.eu/eurostat/statistics-explained/index.php/Natural_gas_price_statistics > [accessed March 5, 2018].